Dijlah Journal of Medical Sciences (DJMS) Vol. 3, No. 3, September, 2026, pp. 129-142
P-ISSN: 3078-3178, E-ISSN: 3078-8625, paper ID: 11

ORIGINAL ARTICLE

Advanced MRI Assessment of Ovarian Torsion: A Pilot Surgical-Correlation Study of Ischemic Severity and Ovarian Viability

Saradiq Mudhafar Jebur[1*] and Mohammed Ali Alalsaidiessa[2]
[1]Department of Radiology Technologies, College of Health and Medical Technologies, Dijlah University, Baghdad, Iraq
[2]Radiology Department, Medical City, Baghdad Teaching Hospital, Baghdad, Iraq

Article Info

Article history:

Received June, 09, 2026
Revised June, 23, 2026
Accepted July, 02, 2026

Keywords:

Ovarian Torsion,
Magnetic Resonance Imaging,
Diffusion Weighted Imaging,
Apparent Diffusion Coefficient,
3D-CISS,
Susceptibility Weighted Imaging,
Ovarian Viability,
Surgical Correlation

ABSTRACT

To assess whether adding advanced MRI sequences, including diffusion-weighted imaging (DWI), apparent diffusion coefficient (ADC) mapping, three-dimensional constructive interference in steady state (3D-CISS), and susceptibility-weighted imaging (SWI), improves twisted pedicle visualization and supports assessment of ovarian viability in surgically confirmed ovarian torsion. This prospective pilot surgical-correlation study included 30 female patients presenting with acute lower abdominal or pelvic pain. All of them were later confirmed, during surgery, to have ovarian torsion. The study was carried out at Private Nursing Home Hospital in Baghdad, Iraq, from 1st April 2026 to 7th June 2026. All patients underwent pelvic MRI on a 1.5 T system during the emergency imaging workup. Routine MRI included T1-weighted, T2-weighted, and post-contrast fat-suppressed sequences when contrast was clinically permitted. DWI, ADC mapping, 3D-CISS, and SWI were then added as the advanced protocol. Two radiologists reviewed the images independently while blinded to the operative findings. MRI findings were correlated with intraoperative assessment of ovarian viability. Since only surgically confirmed torsion cases were included, specificity, positive predictive value, negative predictive value, and overall diagnostic accuracy were not calculated. The twisted pedicle was seen more often after adding the advanced sequences, increasing from 40.0% on routine MRI to 83.3% on advanced MRI. Diffusion restriction was present in 27 patients (90.0%) and was seen in all surgically non-viable ovaries. Mean ADC values were lower in non-viable ovaries than in viable ovaries (0.78 ± 0.10 vs. $1.21 \pm 0.15 \times 10^{-3}$ mm²/s; $p < 0.01$). An ADC value $\leq 0.9 \times 10^{-3}$ mm²/s was associated with intraoperative non-viability, although it was treated only as an exploratory marker of ischemic severity rather than a validated cutoff. Inter-observer agreement was excellent for ovarian enlargement, diffusion restriction, and twisted pedicle visualization. In this pilot surgical-correlation study, advanced MRI added useful information beyond routine pelvic MRI in confirmed ovarian torsion. DWI with ADC mapping and 3D-CISS were the most useful additions, improving pedicle visualization and supporting assessment of ischemic severity. The proposed ADC threshold should remain cautious and needs external validation before broader clinical use.

Corresponding Author:

* Saradiq Mudhafar Jebur
Department of Radiology Technologies, College of Health and Medical Technologies, Dijlah University, Baghdad, Iraq
Email: saradiq.mudafar@duc.edu.iq

1- INTRODUCTION

Ovarian torsion is a gynecological emergency that demands prompt recognition, since any delay can directly threaten the ovary's survival. The condition arises when the ovary and at times the fallopian tube on the same side rotates around its vascular pedicle. This typically starts quietly, with venous and lymphatic drainage becoming obstructed first. As the obstruction persists, the ovarian stroma grows edematous and congested, and hemorrhage may follow. Left untwisted, the torsion can eventually choke off arterial supply as well, at which point the ischemic damage becomes irreversible. Ovarian torsion makes up only a small fraction of acute pelvic presentations, yet its consequences when missed are disproportionately serious. A delayed diagnosis can cost a patient her ovary through necrosis and, ultimately, an oophorectomy that might otherwise have been avoided along with the fertility potential tied to it. The stakes are especially high in adolescents and women still within their reproductive years [1, 2]. The clinical picture rarely makes the diagnosis straightforward. Patients can show up with pain that is sudden or comes and goes, along with nausea, vomiting, tenderness on adnexal exam, and sometimes a mild rise in white cell count or other inflammatory markers. None of this is specific the same constellation could just as easily point to appendicitis, a ruptured ovarian cyst, renal colic, pelvic inflammatory disease, or an ectopic pregnancy. Clinical judgment alone, then, often falls short. This is exactly where imaging needs to carry more weight than simply flagging that "something is wrong" with the adnexa. Ideally, it should raise the suspicion of torsion itself, pin down the twisted pedicle when that's possible, and offer some sense of whether the ovary is still viable. None of this is academic surgeons making this call are working against the clock [3, 4].

Ultrasonography remains the first-line imaging modality for suspected ovarian torsion due to its speed, accessibility, low cost, and lack of ionizing radiation. Typical sonographic findings include ovarian enlargement, stromal edema, peripheral follicular arrangement, free pelvic fluid, and sometimes the whirlpool sign of a twisted vascular pedicle. However, ultrasound has important limitations. Doppler flow may be preserved despite torsion because of dual ovarian arterial supply, partial torsion, or intermittent twisting. Therefore, preserved arterial or venous flow cannot safely exclude torsion [5, 6]. CT may show secondary findings in patients scanned for acute abdominal pain, including adnexal enlargement, uterine deviation, fat stranding, or hemorrhagic components. However, CT is not primarily designed for ovarian viability assessment, and radiation exposure remains a concern, particularly in young patients [7, 8]. MRI provides better soft-tissue characterization. It can show ovarian enlargement, stromal edema, hemorrhage, tubal thickening, twisted pedicle morphology, enhancement pattern, and associated pelvic fluid. Previous MRI research has shown that if irreversible ischemia has not yet occurred, a torsed ovary may remain viable even when significantly enlarged [9, 10]. More recent work also supports MRI as a problem-solving modality after equivocal ultrasound, particularly in children and adolescents, where diagnostic certainty must be balanced against radiation avoidance and surgical urgency [11, 12]. Yet a practical gap persists. Most pelvic MRI protocols still lean heavily on the conventional trio T1, T2, and post-contrast sequences. These are valuable, but they weren't built to capture the early physiological cascade that torsion sets off. A radiologist working with them can usually spot an enlarged ovary, displaced follicles, or odd enhancement, yet still walk away unsure whether the pedicle is actually twisted or whether the tissue underneath is salvageable. This is the gap advanced sequences are positioned to close. DWI paired with ADC mapping picks up restricted diffusion, a fairly direct signature of ischemic injury. For the pedicle itself, high-resolution steady state imaging 3D-CISS being the prime example offers a sharper look at the twist and the whirlpool pattern it creates. And SWI adds yet another layer, catching hemorrhagic or venous congestive change that often slips past on the standard sequences [13, 14, 15].

The exact added value of these advanced MRI sequences in ovarian torsion is still not fully standardized. Many studies describe general MRI appearances or compare MRI with ultrasound and CT, but fewer studies evaluate DWI, ADC mapping, high-resolution pedicle imaging, and susceptibility-based assessment together within one emergency MRI workflow. Even fewer correlate these findings directly with intraoperative ovarian viability. Therefore, the present pilot surgical-correlation study was designed to evaluate the added value of advanced MRI sequences, mainly DWI, ADC mapping, 3D-CISS, and SWI, in surgically confirmed ovarian torsion. The aim was to assess whether these sequences improve twisted pedicle visualization and support exploratory evaluation of ischemic severity and ovarian viability within a feasible 1.5 T emergency MRI protocol.

2- MATERIALS AND METHODS

2.1 Study Design and Setting

This prospective pilot surgical-correlation study was carried out at Private Nursing Home Hospital, Baghdad, Iraq. The hospital receives gynecologic emergency cases and provides cross-sectional imaging services. The study was conducted from 1st April 2026 to 7th June 2026. All female patients who presented to the emergency department with acute lower abdominal or pelvic pain and clinical or ultrasound suspicion of ovarian torsion were screened for inclusion. The study was designed to evaluate the added value of advanced MRI sequences in surgically confirmed ovarian torsion. The main evaluated points were twisted pedicle visualization, ischemic imaging changes, hemorrhagic congestion, and intraoperative ovarian viability. Surgical findings were used as the reference standard for confirming torsion and assessing ovarian viability. Because the study included only patients with surgically confirmed torsion, it was not designed as a full diagnostic accuracy study. Non-torsion controls were not included because the primary aim was not to distinguish torsion from other pelvic emergencies, but to correlate MRI findings with surgical viability among confirmed torsion cases. Therefore, specificity, positive predictive value, negative predictive value, and overall diagnostic accuracy were not calculated.

2.2 Study Population

Thirty consecutive female patients were included. All patients had suspected ovarian torsion before surgery, underwent pelvic MRI before operative intervention, and then had torsion confirmed intraoperatively. Eligibility hinged on a fairly broad clinical picture: acute pelvic pain, adnexal tenderness, nausea or vomiting, or ultrasound findings pointing toward adnexal enlargement, a peripheral arrangement of follicles, altered stromal echogenicity, or a suspected twisted pedicle. From there, four conditions had to be met for actual inclusion female patients between 13 and 58 years old, an emergency presentation with suspected torsion, completion of both the routine and advanced MRI sequences prior to surgery and surgical confirmation via laparoscopy or laparotomy.

A few situations took patients out of the study regardless: confirmed pregnancy, a prior adnexectomy on the same side, known pelvic malignancy, motion artifact severe enough to compromise MRI interpretation, any contraindication to MRI, or operative documentation that was incomplete. Pregnancy itself was ruled out through routine β-hCG testing as part of the standard emergency workup. Beyond that, anyone with incomplete MRI sequences or no available operative viability assessment was excluded as well.

2.3 Ethical Considerations

The study protocol was approved by the local ethics committee of Private Nursing Home Hospital. Written informed consent was obtained from all adult participants. For patients younger than 18 years, consent was obtained from a parent or legal guardian, with patient assent when clinically possible. The study followed the principles of the Declaration of Helsinki. No additional invasive procedure was performed for research purposes, and all imaging and surgical data were anonymized before analysis.

2.4 MRI Acquisition Protocol

All scanning was carried out on a Philips Achieva 1.5T system with a phased-array pelvic coil, patients lying supine throughout. Where it was clinically feasible, patients fasted for at least four hours beforehand and partially emptied their bladder, and anti-peristaltic medication was given provided there was no contraindication following the department's usual practice to settle bowel motion and sharpen pelvic visualization. Without repositioning the patient, each examination ran through two protocols back-to-back. The routine one covered axial T1-weighted spin-echo, T2-weighted fast spin-echo in both axial and coronal planes, and post-contrast fat-suppressed T1-weighted imaging whenever contrast was clinically appropriate. Together, these sequences carried the bulk of the assessment: ovarian enlargement, stromal edema, and the arrangement of peripheral follicles, hemorrhagic signal, pelvic fluid, and the enhancement pattern. Contrast itself was reserved for patients with acceptable renal function, no history of contrast allergy, and a clinical status that allowed for it without holding up surgery. Anyone who didn't meet those conditions was simply assessed on the non-contrast routine sequences alongside the advanced non-contrast set. The advanced protocol brought together DWI with ADC mapping, 3D-CISS, and SWI. DWI was run as single-shot echo-planar imaging at b-values of 0 and 800 s/mm², with ADC maps generated automatically from there. The choice of 800 s/mm² wasn't arbitrary it's a value widely used in pelvic emergency imaging precisely because it strikes a workable balance between diffusion weighting, signal-to-noise, and scan time at 1.5T. Pushing to higher or multiple b-values might sharpen the diffusion model, but in an emergency, cohort already pressed for time, the added scan length and motion sensitivity weren't worth the trade-off. DWI and ADC were included in the first place because restricted diffusion can flag ischemic ovarian injury, a use supported by earlier MRI work on detecting hemorrhagic infarction in torsion [16]. 3D-CISS, acquired as thin sections with multi-planar reconstruction, was there specifically to sharpen the view of the twisted pedicle and its whirlpool pattern, while SWI handled the job of picking up hemorrhage, venous congestion, and susceptibility blooming. Both protocols together took roughly 25–30 minutes, and parallel imaging was used whenever available to keep scan time down and limit motion-related degradation.

2.5 Image Interpretation

All MRI datasets were anonymized and reviewed on the hospital PACS. Two radiologists with experience in pelvic MRI independently evaluated the images. Both readers were blinded to the operative findings at the time of interpretation. Routine MRI sequences and advanced MRI sequences were assessed separately to reduce interpretive bias. Any disagreement was resolved later by consensus review. For each case, the following findings were recorded: ovarian enlargement, stromal T2 hyper-intensity, peripheral follicular arrangement, twisted pedicle or whirlpool sign, uterine deviation toward the affected side, pelvic fluid, hemorrhagic signal on T1-weighted or SWI images, post-contrast enhancement pattern, diffusion restriction, and ADC value. Ovarian enlargement was defined as a maximum ovarian diameter greater than 4 cm or clear asymmetry compared with the contralateral ovary. Stromal edema was recorded when the affected ovary showed increased or heterogeneous T2 signal. The twisted pedicle, or whirlpool sign, was defined as a coiled vascular or tubular structure adjacent to the affected adnexa, especially when confirmed on multi-planar 3D-CISS images. Diffusion restriction was defined as high signal intensity on high-b-value DWI with corresponding low signal on the ADC map. Post-contrast enhancement was classified as preserved, reduced, absent, or rim-like. Rim-like enhancement was defined as thin peripheral enhancement with poor or absent central stromal enhancement of the affected ovary. SWI findings were recorded using a simple three-point visual score: 0 = no blooming or hemorrhagic susceptibility signal, 1 = mild focal blooming and 2 = moderate to marked blooming or diffuse hemorrhagic susceptibility signal. For statistical analysis, SWI blooming was also dichotomized as absent or present.

2.6 ADC Measurement

ADC values were measured manually on the generated ADC maps. A region of interest (ROI) was placed within the ovarian stroma of the affected ovary, using the largest possible solid stromal area that could be measured without including visible follicles, hemorrhagic areas, cystic components, or motion-related artifacts. These areas were avoided because they may falsely alter ADC measurements and reduce measurement reliability. When image quality allowed, three separate stromal ADC measurements were obtained from the affected ovary, and the mean value was used for analysis. ROI placement was performed by the primary reader and reviewed by the second reader during consensus assessment. The approximate ROI size was kept as consistent as possible between cases, while still adapting to ovarian size and available stromal tissue. ADC values were reported as $\times 10^{-3}$ mm²/s. An ADC value of $\leq 0.9 \times 10^{-3}$ mm²/s was considered suggestive of marked diffusion restriction. This value was not used as an independent diagnostic criterion because the study was small and exploratory. It was assessed only as a supportive imaging marker in relation to intraoperative ovarian viability. The use of DWI and ADC mapping in adnexal torsion has been previously reported as useful for detecting ischemic-related diffusion restriction and supporting assessment of ovarian injury [4, 5].

2.7 Surgical Reference Standard

All included patients underwent emergency surgical exploration by laparoscopy or laparotomy. The surgical approach was determined by the gynecology team according to clinical urgency, patient condition, and intraoperative findings. Surgical records were reviewed for the side of torsion, number of pedicle twists when documented, gross ovarian color, congestion, hemorrhage, associated adnexal lesion, detorsion attempt, ovarian preservation, oophorectomy, or salpingo-oophorectomy. Ovarian viability was classified intraoperatively as viable or non-viable. Viable ovaries were defined as ovaries that showed recovery of color, improvement in perfusion, reduction of congestion, or preserved bleeding response after detorsion, and were therefore preserved. Non-viable ovaries were defined as ovaries described intraoperatively as frankly necrotic or gangrenous, or ovaries showing no meaningful recovery of color or perfusion after detorsion, leading to oophorectomy or salpingo-oophorectomy.

When ovarian tissue was removed, histopathology findings were reviewed to support the surgical assessment. The intraoperative assessment was used as the reference standard because it remains the most direct practical method for confirming torsion and assessing ovarian viability in emergency settings. However, this assessment is partly subjective and may vary between surgeons; therefore, ovarian viability was interpreted as an operative reference standard rather than an absolute biological endpoint [3,6].

2.8 Statistical Analysis

Data were analyzed using descriptive and comparative statistics. Continuous variables were first assessed for distribution using the Shapiro-Wilk test. Normally distributed variables were presented as mean ± standard deviation, while non-normally distributed variables were presented as median and range. Categorical variables were reported as numbers and percentages. Detection rates of major MRI findings were compared between routine and advanced MRI protocols. McNemar's test was used for paired categorical comparisons when the same imaging finding could be assessed on both protocols. For comparisons between surgically viable and non-viable ovaries, categorical variables were analyzed using Fisher's exact test because of the small sample size and expected low cell counts. ADC values were compared between surgically viable and non-viable ovaries using an independent-samples t-test when distribution was normal or the Mann-Whitney U test when normality was not confirmed. The relationship between ADC values and the interval from symptom onset to surgery was assessed using Spearman correlation unless both variables showed normal distribution, in which case Pearson correlation was used. Correlation coefficients were interpreted as exploratory because of the limited cohort size. To reduce the risk of false-positive findings from multiple comparisons, p values for secondary imaging comparisons were interpreted cautiously. The main predefined comparisons were twisted pedicle visualization between routine and advanced MRI, and ADC values between surgically viable and non-viable ovaries. Other comparisons were treated as exploratory. When appropriate, 95% confidence intervals were reported for key estimates.

Inter-observer agreement for major MRI findings, including twisted pedicle visualization, diffusion restriction, SWI blooming or hemorrhagic change, and post-contrast enhancement pattern, was assessed using Cohen's kappa coefficient. Agreement was interpreted as slight, fair, moderate, substantial, or excellent according to commonly used kappa interpretation categories. A two-sided p value <0.05 was considered statistically significant for the main predefined comparisons. Because this pilot study included only surgically confirmed ovarian torsion cases and did not include a non-torsion control group, specificity, positive predictive value, negative predictive value, and overall diagnostic accuracy were not calculated. The analysis was therefore performed as a pilot surgical-correlation study rather than a full diagnostic accuracy study.

Table (1): MRI Acquisition Protocol Used in the Study

Sequence / Component	Main purpose
Fasting, partial bladder voiding, and antiperistaltic medication when appropriate	Reduce motion and improve pelvic visualization
Axial T1-weighted spin-echo	Detect hemorrhagic signal and baseline anatomy
Axial and coronal T2-weighted fast spin-echo	Assess ovarian enlargement, stromal edema, follicles, and pelvic fluid
Post-contrast fat-suppressed T1-weighted imaging	Evaluate enhancement pattern when contrast was clinically permitted
DWI, b = 0 and 800 s/mm²	Detect restricted diffusion related to ischemic injury
ADC mapping	Quantitative assessment of diffusion restriction and viability
3D-CISS with multiplanar reconstruction	Improve visualization of twisted pedicle and whirlpool sign
SWI	Detect hemorrhage, venous congestion, and blooming artifacts
Parallel imaging when available	Reduce motion-related degradation and acquisition time

Table (2): ADC Measurement and Surgical Viability Assessment

Parameter	Method / Definition
ADC map	Generated automatically from DWI sequence
ROI placement	Manual ROI placed within the ovarian stroma of the affected ovary
Areas avoided during ROI placement	Visible follicles, hemorrhagic areas, cystic components, and motion-related artifacts
Number of measurements	Three separate measurements when image quality allowed
Final ADC value	Mean value of repeated stromal measurements
ADC unit	$\times 10^{-3}$ mm²/s
Exploratory ADC marker	ADC $\leq 0.9 \times 10^{-3}$ mm²/s
Interpretation of ADC threshold	Supportive marker of marked diffusion restriction, not an independent diagnostic criterion
Surgical reference standard	Emergency laparoscopy or laparotomy
Viable ovary	Recovery of color or perfusion, reduction of congestion, or preserved bleeding response after detorsion
Non-viable ovary	Frank necrosis, gangrenous appearance, or no meaningful recovery after detorsion, leading to oophorectomy or salpingo-oophorectomy
Histopathology	Reviewed when ovarian tissue was excised

3- RESULTS AND DISCUSSION

3.1 Baseline Clinical and Surgical Characteristics

The final analysis included 30 female patients with surgically confirmed ovarian torsion. The mean age was 27.4 ± 9.1 years, with an age range of 13-52 years. Right-sided torsion was more common and was identified in 19 patients (63.3%), while left-sided torsion was identified in 11 patients (36.7%). The mean interval between symptom onset and MRI examination was 10.8 ± 3.6 hours. This interval was not standardized because imaging and surgery were performed according to emergency clinical workflow. Therefore, timing was considered a potential confounding factor when interpreting ADC values and ischemic severity. All MRI examinations included in the analysis were technically adequate for interpretation. In three patients, DWI was repeated immediately because of motion-related ghosting, and the repeated images were accepted for final analysis. Surgical exploration confirmed ovarian torsion in all patients. After detorsion and intraoperative assessment, 16 ovaries (53.3%) were classified as viable and were preserved. The remaining 14 ovaries (46.7%) were classified as non-viable and were treated by oophorectomy or salpingo-oophorectomy according to the surgical decision.

Table (3): Baseline Clinical and Surgical Characteristics of the Study Cohort

Variable	Value
Total patients	30
Age, mean ± SD, years	27.4 ± 9.1
Age range, years	13-52
Right-sided torsion	19 (63.3%)
Left-sided torsion	11 (36.7%)
Mean interval from symptom onset to MRI, hours	10.8 ± 3.6
Technically adequate MRI examinations	30 (100%)
Repeated DWI due to motion-related ghosting	3 (10.0%)
Surgically viable ovaries	16 (53.3%)
Surgically non-viable ovaries	14 (46.7%)

Data are presented as number (%) unless otherwise indicated. SD = standard deviation; DWI = diffusion-weighted imaging. The interval from symptom onset to MRI was not standardized and was considered a potential timing-related confounder when interpreting ADC values and ischemic severity.

3.2 Detection of Key MRI Findings on Routine and Advanced MRI

Ovarian enlargement was identified in all patients on both routine and advanced MRI protocols. Peripheral follicular arrangement was detected in 22 patients (73.3%) on routine MRI and in 24 patients (80.0%) after adding advanced sequences. Stromal T2 hyper-intensity, reflecting edema and venous congestion, was observed in 25 patients (83.3%) on routine MRI and in 27 patients (90.0%) on advanced MRI assessment. The greatest increase was observed in twisted pedicle visualization. Routine MRI showed the twisted pedicle, or whirlpool sign, in 12 patients (40.0%), while advanced MRI, mainly 3D-CISS with multi-planar reconstruction, showed the pedicle in 25 patients (83.3%). This difference was statistically significant ($p < 0.001$). Hemorrhagic or congestive signal abnormality was detected in 14 patients (46.7%) on routine MRI and in 18 patients (60.0%) after adding SWI. Absent or rim-like enhancement was observed in 17 patients (56.7%) on routine MRI and in 22 patients (73.3%) after advanced MRI assessment. Diffusion restriction with low ADC was identified in 27 patients (90.0%) and was assessed only within the advanced MRI protocol. Because this was a pilot surgical-correlation study, secondary imaging comparisons were interpreted cautiously. The main predefined comparison in this part of the analysis was twisted pedicle visualization between routine and advanced MRI.

Table (4): Detection of Key MRI Findings on Routine and Advanced MRI

Imaging finding	Routine MRI	Advanced MRI	p value
Ovarian enlargement	30 (100%)	30 (100%)	—
Peripheral follicular arrangement	22 (73.3%)	24 (80.0%)	0.31
Stromal T2 hyperintensity	25 (83.3%)	27 (90.0%)	0.27
Twisted pedicle / whirlpool sign	12 (40.0%)	25 (83.3%)	<0.001
Hemorrhagic or congestive signal change	14 (46.7%)	18 (60.0%)	0.18
Absent or rim-like enhancement	17 (56.7%)	22 (73.3%)	0.04
Diffusion restriction with low ADC	Not assessed	27 (90.0%)	—

Data are presented as number (%). Advanced MRI included DWI, ADC mapping, 3D-CISS, and SWI. McNemar's test was used for paired categorical comparisons when the same finding could be assessed on both routine and advanced protocols. The main predefined comparison was twisted pedicle visualization between routine and advanced MRI. Other p values were interpreted as exploratory because of the pilot design, limited sample size, and multiple secondary imaging comparisons. ADC = apparent diffusion coefficient; DWI = diffusion-weighted imaging; SWI = susceptibility-weighted imaging.

3.3 Advanced MRI Findings According to Surgical Viability

A clear pattern emerged linking the advanced MRI findings to what surgeons actually found at operation. Every single one of the 14 non-viable ovaries showed diffusion restriction. The ADC cutoff of $\leq 0.9 \times 10^{-3}$ mm²/s told much the same story present in 13 of those 14 non-viable ovaries (92.9%), but in only 2 of the 16 viable ones (12.5%). Enhancement followed a similar split: absent or rim-like patterns showed up in every non-viable ovary, against half of the viable ones (8 of 16, 50.0%). The twisted pedicle itself was visible on advanced imaging in 13 of 14 non-viable cases (92.9%) and in 12 of 16 viable cases (75.0%). SWI blooming or hemorrhagic congestion was less consistent across the board, appearing in 7 non-viable ovaries (50.0%) versus 3 viable ones (18.8%). Taken together these points to diffusion restriction depressed ADC values, and abnormal enhancement tracking non-viability more tightly than morphology alone ever could. That said, the small cohort and the pilot, surgical-correlation nature of the design mean these numbers shouldn't be over-interpreted. The $\leq 0.9 \times 10^{-3}$ mm²/s threshold is best read as an exploratory marker of how severe the ischemia has become not as a diagnostic cutoff that's been validated for clinical use.

Table (5): Advanced MRI Findings According to Surgical Viability

Advanced MRI finding	Viable ovaries (n = 16)	Non-viable ovaries (n = 14)	p value
Twisted pedicle visualized	12 (75.0%)	13 (92.9%)	0.33
Diffusion restriction	13 (81.3%)	14 (100%)	0.23
ADC ≤0.9 $\times 10^{-3}$ mm²/s	2 (12.5%)	13 (92.9%)	<0.001
Absent/rim-like enhancement	8 (50.0%)	14 (100%)	0.004
SWI blooming / hemorrhagic congestion	3 (18.8%)	7 (50.0%)	0.07

Data are presented as number (%). Group comparisons were performed using Fisher's exact test because of the small sample size and expected low cell counts. The ADC threshold of ≤0.9 $\times 10^{-3}$ mm²/s was interpreted as an exploratory supportive marker of ischemic severity, not as a validated diagnostic cutoff. Other p values were interpreted cautiously because of the pilot design and multiple secondary imaging comparisons. ADC = apparent diffusion coefficient; SWI = susceptibility-weighted imaging.

3.4 ADC Values According to Surgical Viability

Mean ADC values differed between viable and non-viable ovaries. Viable ovaries showed a mean ADC value of 1.21 ± 0.15 $\times 10^{-3}$ mm²/s, with a range of 1.05-1.42 $\times 10^{-3}$ mm²/s. Non-viable ovaries showed a lower mean ADC value of 0.78 ± 0.10 $\times 10^{-3}$ mm²/s, with a range of 0.61-0.91 $\times 10^{-3}$ mm²/s. The difference between the two groups was statistically significant ($p < 0.01$). An ADC value of ≤0.9 $\times 10^{-3}$ mm²/s was associated with intraoperative non-viability. However, this value was interpreted as an exploratory supportive marker of ischemic severity rather than an isolated diagnostic rule, because the study was exploratory and included a limited number of patients. An inverse association was observed between ADC values and the interval from symptom onset to surgery. Lower ADC values were more common in patients with longer surgical delay and intraoperative non-viability. Correlation analysis showed a strong negative relationship between ADC value and surgical delay ($r = -0.74$, $p < 0.01$). This relationship was interpreted cautiously because timing from symptom onset to imaging and surgery was not standardized and may have acted as a confounding factor. Still, the finding suggests that ADC may serve as a time-sensitive imaging marker of ischemic severity in ovarian torsion, especially when interpreted together with enhancement pattern, twisted pedicle visualization, and intraoperative findings.

Table (6): ADC Values According to Surgical Viability

Surgical outcome	No. of ovaries	Mean ADC ± SD $\times 10^{-3}$ mm²/s	Range $\times 10^{-3}$ mm²/s	Interpretation
Viable / preserved	16	1.21 ± 0.15	1.05-1.42	Less severe or potentially reversible ischemic change
Non-viable / necrotic	14	0.78 ± 0.10	0.61-0.91	Marked diffusion restriction
p value	—	<0.01	—	Difference between viable and non-viable ovaries

ADC = apparent diffusion coefficient; SD = standard deviation. ADC values were measured in the ovarian stroma, avoiding visible follicles, hemorrhagic areas, cystic components, and motion-related artifacts. The ADC difference between viable and non-viable ovaries was statistically significant, but the proposed ADC threshold of ≤0.9 $\times 10^{-3}$ mm²/s was treated as an exploratory supportive marker rather than a validated diagnostic cutoff.

3.5 Interobserver Agreement

Interobserver agreement was excellent for the most reproducible MRI findings. Agreement was highest for ovarian enlargement (κ = 0.92), followed by diffusion restriction (κ = 0.89) and twisted pedicle / whirlpool sign visualization (κ = 0.87). Agreement for post-contrast enhancement pattern was substantial (κ = 0.75), and agreement for SWI blooming or hemorrhagic change was also substantial (κ = 0.72). Disagreement occurred in 4 cases (13.3%), mainly due to borderline twisted pedicle visualization and subtle enhancement abnormalities. All discrepant cases were resolved by consensus review.

Table (7): Interobserver Agreement for Major MRI Findings

Imaging finding	Cohen's κ	Interpretation
Ovarian enlargement	0.92	Excellent
Diffusion restriction	0.89	Excellent
Twisted pedicle / whirlpool sign	0.87	Excellent
Post-contrast enhancement pattern	0.75	Substantial
SWI blooming / hemorrhagic change	0.72	Substantial

κ = Cohen's kappa coefficient; SWI = susceptibility-weighted imaging. Agreement was interpreted according to commonly used kappa categories.

The present pilot surgical-correlation study showed that advanced MRI sequences can add useful information in surgically confirmed ovarian torsion. The value was not merely in demonstrating ovarian enlargement, as this finding was present in all patients and, alone, did not address the critical clinical question. The more relevant issue was whether MRI could better define the twisted pedicle and provide an impression of ischemic severity. In this study, advanced MRI improved twisted pedicle visualization from 40.0% on routine MRI to 83.3% after adding advanced sequences, mainly 3D-CISS with multiplanar reconstruction. DWI and ADC mapping also helped separate viable from non-viable ovaries. These findings are consistent with previous MRI-pathology correlation work showing that hemorrhagic infarction and viability can be reflected by MRI appearances. Moribata et al. reported that MRI findings in ovarian torsion correlate with pathological hemorrhagic infarction, supporting the idea that MRI may reflect not only morphology but also the stage of tissue injury [18]. In the present study, ovarian enlargement and stromal T2 hyperintensity were common, but they did not clearly separate viable from non-viable ovaries. Thus, routine morphologic signs are useful for raising suspicion of torsion, but less reliable for judging the biological stage of ischemia. The increase in twisted pedicle visualization was one of the strongest observations in this study. The twisted pedicle is a direct sign of torsion, but it may be difficult to identify on routine T1- and T2-weighted images, especially when the ovary is enlarged, displaced, or surrounded by fluid. Singh et al. described a broad spectrum of MRI findings in ovarian torsion, including pedicle-related and hemorrhagic features [19]. Our results add to this point by suggesting that thin-section 3D-CISS with multiplanar reconstruction may make the twisted pedicle more visible within an emergency MRI protocol.

The pediatric and adolescent context also matters, although the present cohort was not limited to children. Ovarian torsion can be diagnostically difficult in younger patients because symptoms may be vague, clinical examination may be limited, and preservation of ovarian function is especially important. Ngo et al. emphasized the wide imaging spectrum of pediatric ovarian torsion and the need to recognize findings beyond a single sign [20]. In this study, advanced MRI was helpful because it combined pedicle assessment with diffusion and susceptibility-based findings. Similarly, Sintim-Damoa *et al*. described the variable imaging spectrum of pediatric ovarian torsion and highlighted that imaging findings may overlap with other adnexal or pelvic conditions [21]. This overlap is relevant to the present study because ovarian enlargement, pelvic fluid, and stromal edema were frequent but not specific markers of non-viability. The current results therefore support a pattern-based approach rather than reliance on one sign. DWI and ADC mapping provided another level of assessment. Non-viable ovaries had lower ADC values than viable ovaries, and an ADC value of $\leq 0.9 \times 10^{-3}$ mm²/s was strongly associated with intraoperative non-viability. Lee et al., in a systematic review and meta-analysis, supported the diagnostic value of MRI in adnexal torsion, although the available evidence remains limited by heterogeneity among studies [22]. In our cohort, ADC seemed to help

MRI move from simple anatomical description toward a more functional estimate of ischemic severity. The inverse association between ADC values and surgical delay supports this interpretation, but it should not be over-read. Torsion is not a fixed event; it progresses from venous and lymphatic obstruction to edema, congestion, impaired perfusion, and sometimes irreversible ischemia. Still, ADC can be affected by hemorrhage, cystic areas, ROI placement, motion artifact, and technical factors. The ACOG Committee Opinion also emphasizes that adnexal torsion remains a clinical and surgical emergency, and management should not depend on imaging alone [23]. For this reason, ADC should be interpreted together with enhancement pattern, pedicle visualization, SWI findings, and the operative context.

SWI had a supportive role in this study. Blooming or hemorrhagic congestion was more common in non-viable ovaries, but it was not present in every case. This is expected because susceptibility findings depend on blood products, venous congestion, and hemorrhagic change, which vary according to the duration and severity of torsion. Childress and Dietrich discussed the variable clinical and imaging findings of pediatric ovarian torsion and emphasized timely management to preserve ovarian function when possible [24]. In the present study, SWI increased confidence when positive, especially when low ADC and absent or rim-like enhancement were also present. Post-contrast imaging earned its place in the protocol, but it can't carry the diagnosis on its own. Every non-viable ovary in this cohort showed absent or rim-like enhancement, which fits the idea that poor enhancement tracks reduced perfusion and more advanced ischemic damage. Still, enhancement isn't a clean signal timing, partial torsion, intermittent detorsion, and leftover peripheral blood flow can all shift it. Robertson et al. made a similar point in their discussion of common misconceptions around evaluating and managing ovarian torsion, warning specifically about the false reassurance that incomplete clinical or imaging findings can produce [25]. The takeaway here is the same: no single MRI sign deserves to be treated as the final word.

Ultrasound, for its part, hasn't lost its position as the first-line test it's quick, widely available, safe, and cheap. But its blind spot is well documented: Doppler flow can look perfectly preserved even when torsion is present. Wilkinson and Sanderson framed adnexal torsion as fundamentally a multimodality imaging problem, where ultrasound, CT, and MRI each pull their weight depending on the clinical situation [26]. Nothing in the present findings argues for replacing ultrasound as the initial step. MRI's value shows up later in the workflow when ultrasound leaves things unresolved, when the anatomy is awkward to read, or when the question shifts specifically to whether the ovary is still viable. The use of susceptibility-based sequences may also deserve more attention. Takeuchi et al. described the value of susceptibility-weighted MR sequences in evaluating ovarian masses with torsion, especially for detecting hemorrhagic components [27]. This supports the role of SWI in the present study as an adjunctive sequence. Still, SWI should remain supportive rather than definitive. It may strengthen interpretation when positive, but it cannot replace DWI/ADC, enhancement assessment, or surgical judgment. The practical implication is that in suspected torsion, the radiologist should not rely solely on identifying ovarian enlargement. A more useful report should define the twisted pedicle when visible, describe diffusion restriction and ADC values, comment on enhancement pattern when contrast is available, and mention hemorrhagic or congestive susceptibility findings when present. This more integrated interpretation may support surgical decision-making, while still respecting that final viability assessment remains operative [28].

This study has several limitations. First, the sample size was small, with only 30 patients from a single center. Therefore, the results should be interpreted as preliminary and hypothesis-generating. A formal prospective power calculation was not performed, which limits the strength of statistical inference, particularly for subgroup comparisons. Second, all included patients had surgically confirmed ovarian torsion. This design was appropriate for surgical correlation but prevents calculation of specificity, positive predictive value, negative predictive value, and overall diagnostic accuracy. Non-torsion controls were not included, so the findings cannot be generalized as a full diagnostic accuracy model. Third, the ADC threshold of $\leq 0.9 \times 10^{-3}$ mm²/s was derived from this limited cohort and should not be considered a validated cutoff. It may vary across institutions, scanner vendors, sequence parameters, ROI methods, and field strengths. External validation and, ideally, ROC-based threshold analysis in larger cohorts are required. Fourth, timing from symptom onset to MRI and surgery was not standardized. This is important because ADC values and enhancement patterns may change over time as torsion progresses. In this pilot sample, timing could not be fully isolated from viability status by multivariable modeling. Fifth, contrast-enhanced imaging was performed only when clinically permitted. This may introduce selection bias in the interpretation of enhancement patterns. The number of patients receiving contrast and the reasons for non-administration should be stated clearly if available. Sixth, intraoperative viability assessment was used as the reference standard, but it remains partly subjective and may vary between surgeons. Histopathology was available only when ovarian tissue was excised. Finally, long-term ovarian function, fertility outcome, and recurrence were not assessed. Larger multicenter studies with standardized MRI protocols and clinical follow-up are needed.

4- CONCLUSION

Advanced MRI sequences, particularly DWI with ADC mapping and 3D-CISS, added clinically relevant information beyond routine pelvic MRI in this pilot surgical-correlation study of ovarian torsion. These sequences improved twisted pedicle visualization and supported exploratory assessment of ischemic severity and ovarian viability. SWI provided additional supportive information when hemorrhagic congestion was present. The ADC threshold of $\leq 0.9 \times 10^{-3}$ mm²/s should be considered exploratory and requires external validation before wider clinical use.

Figure Legends

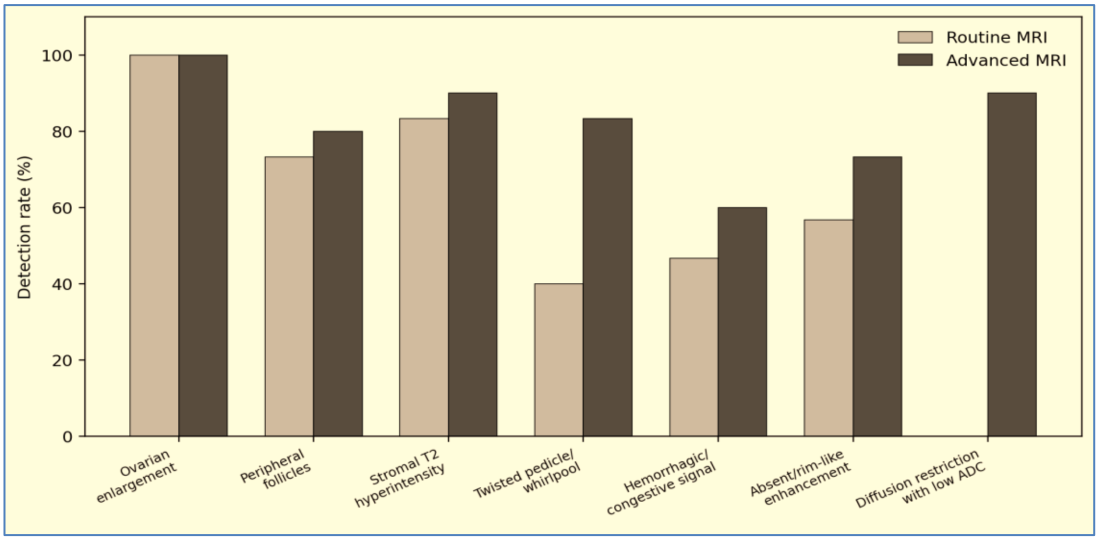

Fig (1): Detection rates of major MRI findings on routine and advanced MRI. Bar chart comparing detection rates of key MRI findings between routine MRI and advanced MRI. The largest increase was observed for twisted pedicle visualization, increasing from 40.0% to 83.3% after adding advanced MRI sequences. Diffusion restriction with low ADC was assessed only in the advanced MRI protocol

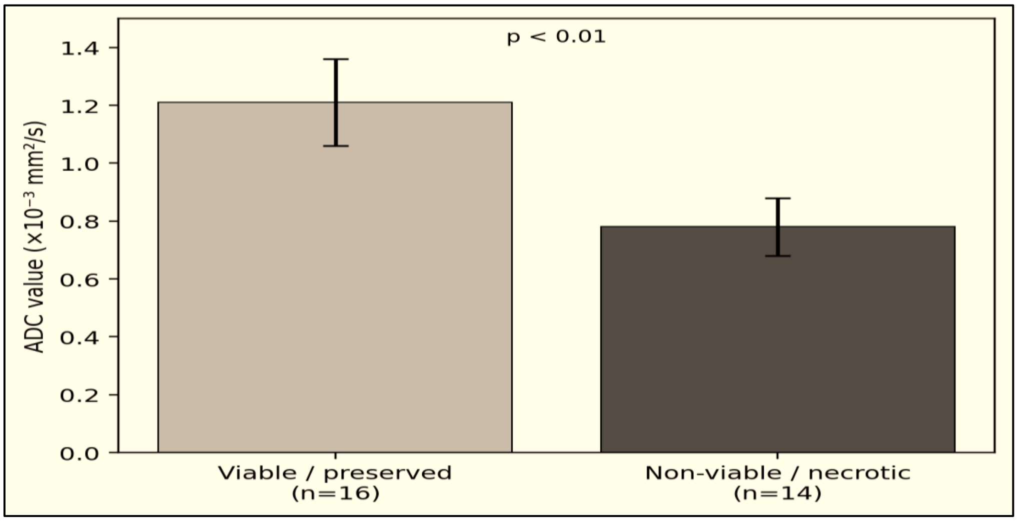

Fig (2): ADC values according to surgical viability. Bar-chart showing means ADC values according to surgical viability. Non-viable ovaries showed significantly lower mean ADC values than viable ovaries. Error bars represent standard deviation. Mean ADC was $1.21 \pm 0.15 \times 10^{-3}$ mm²/s in viable ovaries and $0.78 \pm 0.10 \times 10^{-3}$ mm²/s in non-viable ovaries ($p < 0.01$)

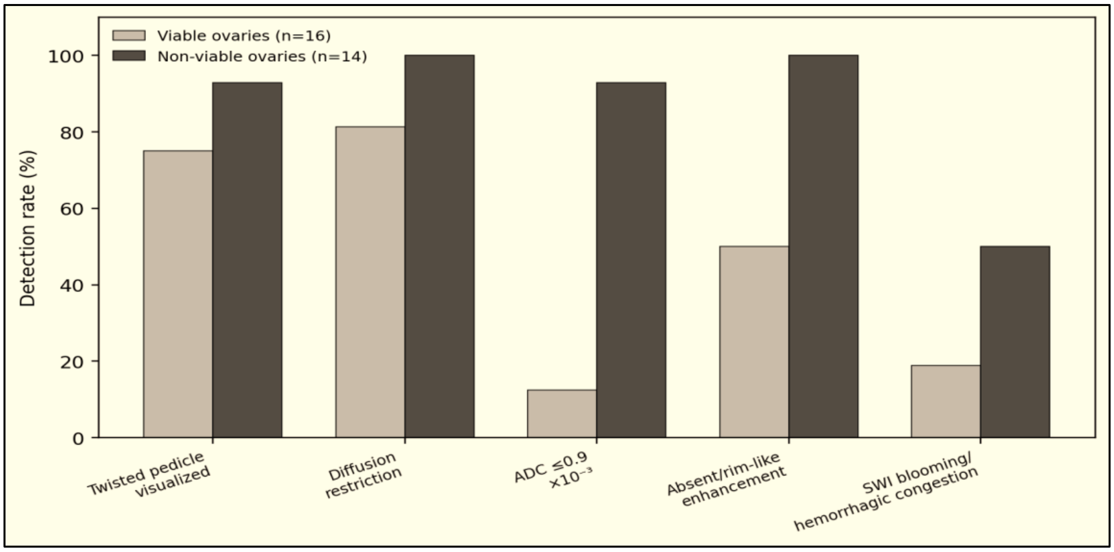

Fig (3): Advanced MRI findings according to ovarian viability. Grouped bar chart comparing advanced MRI findings between viable and non-viable ovaries. ADC ≤0.9 $\times 10^{-3}$ mm²/s and absent/rim-like enhancement were more frequent in non-viable ovaries, while SWI blooming/hemorrhagic congestion showed a positive but less consistent association

REFERENCES

[1] Dawood, M. T., Naik, M., Bharwani, N., Sudderuddin, S. A., Rockall, A. G., and Stewart, V. R. (2021). Adnexal torsion: Review of radiologic appearances. *Radiographics*, *41*(2), 609–624. https://doi.org/10.1148/rg.2021200118

[2] Strachowski, L. M., Choi, H. H., Shum, D. J., and Horrow, M. M. (2021). Pearls and pitfalls in imaging of pelvic adnexal torsion: Seven tips to tell it's twisted. *Radiographics*, *41*(2), 625–640. https://doi.org/10.1148/rg.2021200122

[3] Béranger-Gibert, S., Sakly, H., Ballester, M., Rock, A., Akl, S., Bazot, M., and Thomassin-Naggara, I. (2016). Diagnostic value of MR imaging in the diagnosis of adnexal torsion. *Radiology*, *279* (2), 461–470. https://doi.org/10.1148/radiol.2015150261

[4] Akçay, A., Gültekin, M. A., and Altıntaş, F. (2025). Magnetic resonance imaging characteristics of ovarian torsion: Insights into diagnostic features. *Abdominal Radiology*, *50*(6), 2694–2702. https://doi.org/10.1007/s00261-024-04702-0

[5] Fujii, S., Kaneda, S., Kakite, S., Kanasaki, Y., Matsusue, E., Harada, T., et al. (2011). Diffusion-weighted imaging findings of adnexal torsion: Initial results. *European Journal of Radiology*, *77*(2), 330–334. https://doi.org/10.1016/j.ejrad.2009.07.040

[6] Petkovska, I., Duke, E., Martin, D. R., Irani, Z., Schabel, K. J., Javitt, M. C., and Katz, D. S. (2016). MRI of ovarian torsion: Correlation of imaging features with the presence of perifollicular hemorrhage and ovarian viability. *European Journal of Radiology*, *85* (11), 2064–2071. https://doi.org/10.1016/j.ejrad.2016.09.020

[7] Duigenan, S., Oliva, E., and Lee, S. I. (2012). Ovarian torsion: Diagnostic features on CT and MRI with pathologic correlation. *American Journal of Roentgenology*, *198*(2), W122–W131. https://doi.org/10.2214/AJR.10.7293

[8] Lourenco, A. P., Swenson, D., Tubbs, R. J., and Lazarus, E. (2014). Ovarian and tubal torsion: Imaging findings on US, CT, and MRI. *Emergency Radiology*, *21*(2), 179–187. https://doi.org/10.1007/s10140-013-1163-3

[9] Rougier, E., Mar, W., Della Valle, V., Morel, B., Irtan, S., Audureau, E., et al. (2020). Added value of MRI for the diagnosis of adnexal torsion in children and adolescents after inconclusive ultrasound examination. *Diagnostic and Interventional Imaging, 101*(12), 747–756. https://doi.org/10.1016/j.diii.2020.04.015

[10] Garde, I., Rimmer, M. P., and Al Wattar, B. H. (2023). Diagnostic accuracy of ultrasound signs for detecting adnexal torsion: Systematic review and meta-analysis. *Ultrasound in Obstetrics & Gynecology, 61*(3), 310–324. https://doi.org/10.1002/uog.24976

[11] Wattar, B., Rimmer, M., Rogozinska, E., Macmillan, M., Khan, K. S., and Al Wattar, B. H. (2021). Accuracy of imaging modalities for adnexal torsion: A systematic review and meta-analysis. BJOG: An International *Journal of Obstetrics & Gynaecology, 128* (1), 37–44. https://doi.org/10.1111/1471-0528.16371

[12] Ghossain, M. A., Hachem, K., Buy, J. N., Lignières, F., Vadrot, D., and Hugol, D. (2004). Adnexal torsion: Magnetic resonance findings in the viable adnexa with emphasis on stromal ovarian appearance. *Journal of Magnetic Resonance Imaging, 20* (3), 451–462. https://doi.org/10.1002/jmri.20131

[13] Haque, T. L., Togashi, K., Kobayashi, H., Fujii, S., and Konishi, J. (2000). Adnexal torsion: MR imaging findings of viable ovary. *European Radiology, 10* (12), 1954–1957. https://doi.org/10.1007/s003300000461

[14] Rha, S. E., Byun, J. Y., Jung, S. E., Kim, H. H., Lee, H. G., and Lee, J. M. (2002). CT and MR imaging features of adnexal torsion. *Radiographics, 22* (2), 283–294. https://doi.org/10.1148/radiographics.22.2.g02mr02283

[15] Epstein, K. N., Trout, A. T., Debnath, P., Dillman, J. R., Tkach, J. A., Kline-Fath, B. M., et al. (2024). Rapid, free-breathing non-contrast MRI for first-line imaging evaluation of ovarian torsion in the emergency department. *Pediatric Radiology, 54* (2), 228–235. https://doi.org/10.1007/s00247-023-05827-y

[16] Kato, H., Kanematsu, M., Uchiyama, M., Yano, R., Furui, T., and Morishige, K. (2014). Diffusion-weighted imaging of ovarian torsion: Usefulness of apparent diffusion coefficient (ADC) values for the detection of hemorrhagic infarction. *Magnetic Resonance in Medical Sciences, 13*(1), 39–44. https://doi.org/10.2463/mrms.2013-0039

[17] Özdemir, O., Metin, Y., Metin, N. O., and Küpeli, A. (2017). Contribution of diffusion-weighted imaging to conventional MRI for detection of haemorrhagic infarction in ovary torsion. BMC Medical Imaging, 17(1), Article 56. https://doi.org/10.1186/s12880-017-0232-6

[18] Moribata, Y., Kido, A., Yamaoka, T., Mikami, Y., Himoto, Y., Kataoka, M., et al. (2015). MR imaging findings of ovarian torsion correlate with pathological hemorrhagic infarction. Journal of Obstetrics and Gynaecology Research, 41(9), 1433–1439. https://doi.org/10.1111/jog.12717

[19] Singh, T., Prabhakar, N., Singla, V., Bagga, R., and Khandelwal, N. (2018). Spectrum of magnetic resonance imaging findings in ovarian torsion. *Polish Journal of Radiology, 83*, e588–e599. https://doi.org/10.5114/pjr.2018.81157

[20] Ngo, A. V., Otjen, J. P., Parisi, M. T., Ferguson, M. R., Otto, R. K., and Stanescu, A. L. (2015). Pediatric ovarian torsion: A pictorial review. *Pediatric Radiology, 45*(12), 1845–1855. https://doi.org/10.1007/s00247-015-3385-x

[21] Sintim-Damoa, A., Majmudar, A. S., Cohen, H. L., and Parvey, L. S. (2017). Pediatric ovarian torsion: Spectrum of imaging findings. *Radiographics, 37*(6), 1892–1908. https://doi.org/10.1148/rg.2017170026

[22] Lee, J. H., Jeong, Y. K., Park, J. K., and Hwang, J. C. (2020). The diagnostic accuracy of magnetic resonance imaging for adnexal torsion: Systematic review and meta-analysis. *Journal of Clinical Medicine*, 9(7), Article 2209. https://doi.org/10.3390/jcm9072209

[23] American College of Obstetricians and Gynecologists. (2019). Adnexal torsion in adolescents: ACOG Committee Opinion No. 783. *Obstetrics & Gynecology, 1*34(2), e56–e63. https://doi.org/10.1097/AOG.0000000000003373

[24] Childress, K. J., and Dietrich, J. E. (2017). Pediatric ovarian torsion. *Surgical Clinics of North America*, *97*(1), 209–221. https://doi.org/10.1016/j.suc.2016.08.008

[25] Robertson, J. J., Long, B., and Koyfman, A. (2017). Myths in the evaluation and management of ovarian torsion. *Journal of Emergency Medicine*, *52*(4), 449–456. https://doi.org/10.1016/j.jemermed.2016.11.012

[26] Wilkinson, C., and Sanderson, A. (2012). Adnexal torsion: A multimodality imaging review. *Clinical Radiology*, *67*(5), 476–483. https://doi.org/10.1016/j.crad.2011.10.018

[27] Takeuchi, M., Matsuzaki, K., and Harada, M. (2020). Susceptibility-weighted MR sequence for the evaluation of ovarian masses with torsion. *British Journal of Radiology*, 93(1109), Article 20200110. https://doi.org/10.1259/bjr.20200110

[28] Fijean, A. L., Hossu, G., Cherifi, A., Beaumont, M., Morel, O., and Bertholdt, C. (2026). Improving diagnostic accuracy of ovarian torsion using contrast-enhanced ultrasound: A prospective comparative clinical study of performance diagnosis. *International Journal of Gynaecology and Obstetrics*, *172* (2), 1151–1158. https://doi.org/10.1002/ijgo.70429